The Temperature Dependence of the Viscomagnetic Effect

A. L. J. Burgmans *, P. G. van Ditzhuyzen, H. F. P. Knaap, and J. J. M. Beenakker
Kamerlingh Onnes Laboratorium, Rijksuniversiteit, Leiden

(Z. Naturforsch. **28 a**, 835–848 [1973]; received 6th March 1973)

Dedicated to Prof. Dr. L. Waldmann on the occasion of his 60th birthday

A study is presented of the effect of a magnetic field on the viscosity of HD, N_2, CO and CH_4. The temperature dependence of this viscomagnetic effect has been measured in the range between 300 K and the boiling point of these gases. The results are presented in terms of effective cross sections which depend directly on the angle dependent part of the intermolecular potential. The cross sections for reorientation of angular momentum have been compared with those obtained from N.M.R. measurements.

1. Introduction

It is well known that the viscosity of polyatomic gases is influenced by a magnetic field [1, 2]. An explanation of this field effect on dilute polyatomic gases can be given as follows. A velocity gradient in a gas of non-spherical molecules gives rise to an anisotropy not only in the velocities, $\boldsymbol{W}$, but also through collisions in the angular momenta, $\boldsymbol{J}$. This polarization (actually alignment) in the angular momenta can be partially destroyed by the action of a magnetic field (through the Larmor precession). This decreases the polarization in the velocities which changes the transport coefficients.

To describe the viscous behaviour of an isotropic fluid in a magnetic field five shear viscosity coefficients are needed. Until recently the notation used was that of Refs. [3] and [4] where η_1 to η_5 were introduced. As this enumeration is not very expressive we prefer the notation which is introduced by Coope and Snider [5]. They use the elements η_0^+, η_1^+, η_2^+, η_1^- and η_2^- of the real spherical viscosity tensor given by (field in the z direction):

$$\begin{bmatrix} (\frac{3}{2})^{1/2}[\boldsymbol{\Pi}]^{(2)}_{zz} \\ [\boldsymbol{\Pi}]^{(2)}_{xz} \\ [\boldsymbol{\Pi}]^{(2)}_{yz} \\ \frac{1}{2}([\boldsymbol{\Pi}]^{(2)}_{xx} - [\boldsymbol{\Pi}]^{(2)}_{yy}) \\ [\boldsymbol{\Pi}]^{(2)}_{xy} \end{bmatrix} = -2 \begin{bmatrix} \eta_0^+ & 0 & 0 & 0 & 0 \\ 0 & \eta_1^+ & -\eta_1^- & 0 & 0 \\ 0 & \eta_1^- & \eta_1^+ & 0 & 0 \\ 0 & 0 & 0 & \eta_2^+ & -\eta_2^- \\ 0 & 0 & 0 & \eta_2^- & \eta_2^+ \end{bmatrix} \begin{bmatrix} (\frac{3}{2})^{1/2}[\nabla \boldsymbol{v}]^{(2)}_{zz} \\ [\nabla \boldsymbol{v}]^{(2)}_{xz} \\ [\nabla \boldsymbol{v}]^{(2)}_{yz} \\ \frac{1}{2}([\nabla \boldsymbol{v}]^{(2)}_{xx} - [\nabla \boldsymbol{v}]^{(2)}_{yy}) \\ [\nabla \boldsymbol{v}]^{(2)}_{xy} \end{bmatrix} \quad (1)$$

where $[\boldsymbol{\Pi}]^{(2)}_{kl}$ are elements of the symmetric traceless pressure tensor and $[\nabla \boldsymbol{v}]^{(2)}_{kl}$ are elements of the symmetric traceless velocity gradient tensor. The coefficients with a $+$-sign are even, those with a $-$-sign odd functions of the magnetic field. The subscripts 0, 1, 2 refer to the symmetry character of the particular velocity gradients under rotations around the field direction. This notation is also closely related to the notation of Hess and Waldmann [6]. In Table 1 we summarize the relations between the different notations.

Table 1. Identification of the viscosity coefficients as used by different authors.

Coope and Snider [5]	De Groot and Mazur [4]	Hess and Waldmann [6]
η_0^+	η_1	$\eta^{(0)}$
η_1^+	η_3	Re $\eta^{(1)}$
η_2^+	$2\eta_2 - \eta_1$	Re $\eta^{(2)}$
η_1^-	η_5	Im $\eta^{(1)}$
η_2^-	$-\eta_4$	Im $\eta^{(2)}$

Experimentally it has been shown by Hulsman et al. [7–9] that for most simple gases the field effect can be described for all five coefficients by the presence of one type of angular momentum polarization, viz. $[\boldsymbol{J}]^{(2)}$. In this case the experimental results can be characterized by two parameters, one de-

* Present address: Texas A and M University, College Station, Texas, U.S.A.

Reprint requests to Dr. H. F. P. Knaap, Kamerlingh Onnes Laboratorium, Nieuwsteeg 18, *Leiden*, The Netherlands.

scribing the magnitude of the viscosity change and one characterizing the field strength at which the effect occurs. These quantities are related to collision integrals, thus providing direct information on the collisional processes. In particular, the collision integrals obtained are mainly determined by the nonspherical part of the intermolecular interaction.

Up to now nearly all experiments have been performed at room temperature. For a meaningful test of nonspherical potentials it would be very useful to know the temperature dependence of the collision integrals. In the present work such results are given for HD, N_2, CO and CH_4 for temperatures ranging from room temperature down to about the boiling point of these gases.

The results will furthermore be compared with measurements of nuclear magnetic relaxation since these experiments give information concerning the reorientation of the molecules which is similar to that obtained from our experiments.

2. Experimental

2.1. General

As the field effect originates from one type of angular momentum polarization only, the two parameters characterizing the situation can be obtained from any combination of the coefficients η_1^+, η_2^+, η_1^- and η_2^-. Hence the choice of the coefficients to be measured can be determined on the basis of experimental convenience. We use two apparatuses, one (apparatus I) for measurements above 77 K and one (apparatus II) for lower temperatures. Both apparatuses can be considered as a Wheatstone bridge for gas flow, where the resistors are capillaries.

Apparatus I is of the same type as that used by Korving et al.[10]. A capillary of circular cross section (capillary # 1 in Fig. 1) is placed between the poles of a magnent perpendicular to the field direction while the other capillaries are outside the field. On application of the field the viscosity of the gas in the in-field-capillary changes and consequently there is a change in the pressure drop over the capillary. This causes an unbalance of the bridge which is measured with manometer M. From this unbalance one can obtain the viscosity change given by (see also Ref. [10]):

$$\tfrac{1}{2}\,[\eta_1^+ + \eta_2^+ - 2\,\eta(0)] \qquad (2)$$

where $\eta(0)$ is the field free viscosity coefficient.

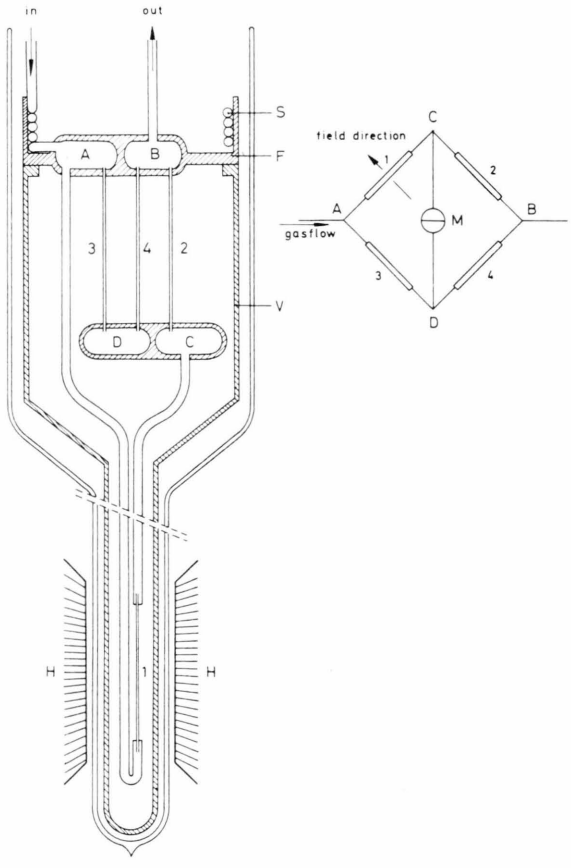

Fig. 1. Schematic diagram of apparatus I for the determination of $\frac{1}{2}[\eta_1^+ + \eta_2^+ - 2\,\eta(0)]$.

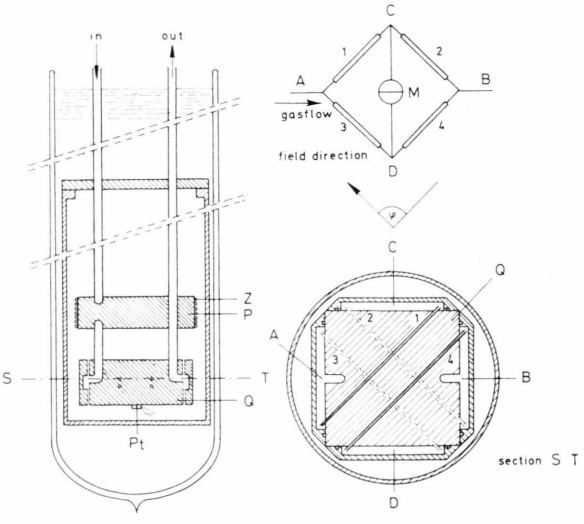

Fig. 2. Schematic diagram of apparatus II for the determination of $\frac{1}{2}(-\eta_1^+ + \eta_2^+)$.

In apparatus II all four capillaries of the bridge are placed in the field, i. e., two parallel and two perpendicular to the field direction (see Figure 2). Since the combination of coefficients measured in a capillary paralel to the field is different from that measured in a capillary perpendicular to the field, a net effect wil result given by (see also Ref. [11]):

$$\tfrac{1}{2}\,(-\eta_1{}^{+}+\eta_2{}^{+}). \qquad (3)$$

2.2. Details

From earlier room temperature work [7–11] it became clear that to obtain a sufficiently constant gasflow through the bridge a good temperature stability is required. Thus it proved necessary to isolate the capillaries by means of a vacuum jacket. In apparatus I this vacuum jacket (V) is quite long (about one meter), which makes it possible to have one capillary in the field and the three others outside the field (see Figure 1). The part of the apparatus inside the vacuum jacket is in thermal contact with the environment through the top flange (F) that also acts as a thermal buffer. The incoming gas is brought to thermal equilibrium in the spiral S, while the volumes A, B, C and D damp out fluctuations in the gasflow. The in-field-capillary has a length of 113 mm and an inner diameter of 1.2 mm.

For measurements at 77 K the apparatus is immersed in a liquid nitrogen bath. Temperatures between 77 K and 293 K are obtained by cooling the vacuum jacket and the top flange with a cold nitrogen vapour stream from a separate dewar. This thermostat is controlled by a Pt thermometer mounted above the top flange (F). In this way a temperature stability of 0.01 K is obtained. The temperature is measured with a Fe-constantan thermal couple on capillary # 1.

Below 77 K it is difficult to achieve a temperature stability good enough to succesfully operate the apparatus described above. For this reason apparatus II was designed in which the vacuum jacket is surrounded by a liquid hydrogen bath. Inside the vacuum jacket higher temperatures than that of liquid hydrogen can be obtained by means of a heater Z (see Figure 2). This heater is wrapped around the thermal buffer P where the temperature of the incoming gas equilibrates while flowing through a spiral inside P. The actual apparatus consists of four capillaries with length 75 mm and inner diameter 0.63 mm, fixed in the brass block Q. In this way a good thermal contact between the capillaries is obtained. Because of the limited field space the construction is as compact as possible. The temperatures are measured with a Pt thermometer (Pt).

The magnet used is an Oerlikon (type C3). The pole pieces for apparatus I have a diameter of 120 mm. With a distance of 50 mm a maximum field of 31.5 kOe can be reached. For apparatus II the maximum field is limited to 22.6 kOe since in that case pole pieces are used of 180 mm diameter at a distance of 120 mm.

In both apparatuses the gasflow through the bridge is adjusted by means of a needle valve upstream and is kept constant by a flow controller (Moore 63 BDL). The pressure in the capillaries can be varied by a valve at the exit of the bridge. The pressures at the points A, B and C are measured with oil manometers. The unbalance of the bridge is measured with a differential membrane manometer with a sensitivity of 10^{-5} Torr (Varian MMM).

The gases used are obtained commercially excepi HD which is prepared using the reaction:

$$\mathrm{LiAlH_4} + 4\,\mathrm{D_2O} \rightarrow \mathrm{LiOD} + \mathrm{Al(OD)_3} + 4\,\mathrm{HD}\,.$$

The small quantities H_2 and D_2 that are present in the product gas are removed using a rectification column as described in Ref. [12]. In Table 2 the purity is given for the gases studied.

Table 2. Purities of the gases studied.

Gas	Purity	Gas	Purity
HD	99.5%	CO	99.95%
N_2	99.9%	CH_4	99.99%

2.3. Consistency tests

By turning the magnet around capillary # 1 of apparatus I the unbalance of the bridge is found to be independent of the orientation of the field. For apparatus II the pressure difference $p_C - p_D$ is a function of the angle φ (see Fig. 2) between the field direction and the direction of one set of capillaries. The dependence of $p_C - p_D$ on φ can be derived from the equation of motion given in Ref. [13] and it is found that:

$$p_C - p_D = (p_C - p_D)_{\varphi=0} \cos 2\varphi\,. \qquad (4)$$

Indeed measurements on a test gas (N_2) as a function of φ can be described by Eq. (4) which is illustrated in Figure 3.

Performing experiments with noble gases, no effect could be detected, as should be expected.

3. Calculation of the Results

In both apparatuses the pressure difference $p_C - p_D$ across the bridge is measured which arises on application of the field. For apparatus I the field

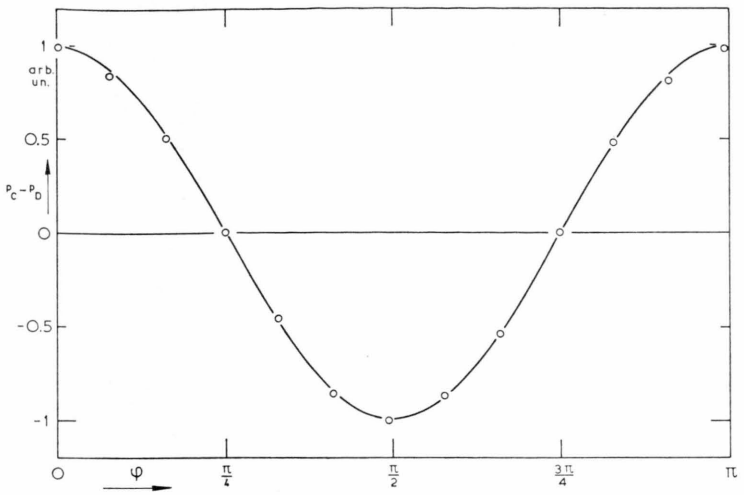

Fig. 3.
The normalized pressure difference $p_C - p_D$ which arises in apparatus II versus the orientation of the magnetic field with respect to the capillaries. The solid line is given by $\cos 2\varphi$ where φ is the angle in Figure 2.

effects are calculated with:

$$-\frac{\eta_1^+ + \eta_2^+ - 2\eta(0)}{2\eta(0)} = 4\frac{p_C - p_D}{p_A - p_B} f \qquad (5)$$

and for apparatus II

$$-\frac{-\eta_1^+ + \eta_2^+}{2\eta(0)} = 2\frac{p_C - p_D}{p_A - p_B} f. \qquad (6)$$

The indices A, B, C and D indicate different points of the bridge (see Figures 1 and 2). The quantity f is a correction factor of the order unity which takes into account the deviations from the ideal Poiseuille flow and the Knudsen effect on the viscosity changes. It is given by:

$$f = \frac{2(p_C + K_\alpha)}{(p_A + K_\alpha) + (p_B + K_\alpha)} \cdot \left[1 + \frac{1}{16}\frac{R}{l}\,\mathrm{Re}(r+s)\right]\left(1 + \frac{K_\beta}{p}\right) \qquad (7)$$

(see also Refs. [8] and [11]).

The factor $2(p_C + K_\alpha)/[(p_A + K_\alpha) + (p_B + K_\alpha)]$ takes into account the expansions of the gas. For apparatus I the expansion factor is usually around 1.3 while for apparatus II this factor is always between 1 and 1.03. The quantity K_α gives the Knudsen correction for the field free flow and can be written as $K_\alpha = n_\alpha p\,\xi/R$, where R is the radius of the capillary, ξ the mean free path of the molecules given by $\xi = (2^{1/2}\pi n \sigma^2)^{-1}$ with n the number density and σ the molecular diameter derived from the field free viscosity, given in Ref. [14]. In accordance with Refs. [15] and [16] it is assumed that n_α has the value 4.

The second factor in Eq. (7) corrects for the extra pressure losses caused by acceleration of the gas at the entrance of the capillary and in the capillary. For both apparatuses this factor is mostly between 1 and 1.01. Here l is the length of the cappilary and Re is Reynolds number equal to $2G/\pi R\eta(0)$ where G is the massflow per unit time through the capillary. The quantity r depends on the shape of the entrance and in accordance with Ref. [15] r is assumed to be 1. The quantity s describes the acceleration of the gas in the capillary. For the two apparatuses s is slightly different since in apparatus I only one capillary is in the field while in apparatus II this is the case for all four capillaries. Consequently for apparatus I the quantity s is given by $s = \ln(p_A/p_C)$ while for aparatus II one has $s = \frac{1}{2}\ln(p_A/p_B)$.

As we work at such low pressures that the mean free path of the molecules is not negligible compared to the diameter of the capillaries, Knudsen effects will reduce the magnitude of the magnetic field effects. A correction is applied by the factor $(1 + K_\beta/p)$. For apparatus I we take $p = \frac{1}{2}(p_A + p_C)$ while for apparatus II we use $p = \frac{1}{2}(p_A + p_B)$. Not only the magnitude of the field effect is affected by Knudsen effects but also the H/p values. Therefore a correction to the experimental H/p values is applied by:

$$H/p = (H/p)_{\mathrm{exp.}}/(1 + K_\gamma/p). \qquad (8)$$

The quantities K_β and K_γ are determined experimentally from an extrapolation to $p = \infty$. For a more detailed discussion see Ref. [8]. The correction factor for the magnitude of the effect is at most 1.4 while

the Knudsen correction for the H/p values is generally small except for HD where the correction factor can be as large as 1.3. Analogous to n_α the numbers n_β and n_γ can be introduced [8] by: $K_{\beta,\gamma} = n_{\beta,\gamma}\, p\, \xi/R$. Within the experimental accuracy these numbers are found to be independent of the temperature and also equal for the two apparatuses. The values found for the different gases are presented in Table 3. The values are in agreement with those obtained in the earlier room temperature measurements [8, 9].

Table 3. Knudsen correction parameters.

	n_α	n_β	n_γ
HD	4	10	14
N_2	4	10	3
CO	4	10	3
CH_4	4	12	2

4. Experimental Results and Discussion

To discuss the experimental results we first give the theoretical expressions derived in Ref. [17] for $[\eta_1^+ + \eta_2^+ - 2\eta(0)]/2\eta(0)$ and $(-\eta_1^+ + \eta_2^+)/2\eta(0)$ based on the $[\boldsymbol{J}]^{(2)}$ polarization which in earlier experiments is found to be dominant:

$$\frac{\eta_1^+ + \eta_2^+ - 2\eta(0)}{2\eta(0)} = -\frac{1}{2}\,\Psi_{02}\left[\frac{\xi_{02}^2}{1+\xi_{02}^2} + \frac{4\,\xi_{02}^2}{1+4\,\xi_{02}^2}\right] \tag{9}$$

and

$$\frac{-\eta_1^+ + \eta_2^+}{2\eta(0)} = -\frac{1}{2}\,\Psi_{02}\left[-\frac{\xi_{02}^2}{1+\xi_{02}^2} + \frac{4\,\xi_{02}^2}{1+4\,\xi_{02}^2}\right] \tag{10}$$

where
$$\Psi_{02} = \mathfrak{S}\left(\tfrac{02}{20}\right)^2/\mathfrak{S}(20)\,\mathfrak{S}(02)\,, \tag{11}$$

$$\xi_{02} = \frac{1}{\langle v_{\mathrm{rel}}\rangle_0\,\mathfrak{S}(02)}\,\frac{g\,\mu_N\,k\,T}{\hbar}\,\frac{H}{p}\,, \tag{12a}$$

$$(H/p)_{\xi_{02}=1} = 2^{1/2}(H/p)_{4/2} = 2^{1/2}(H/p)_{\max} = (\hbar/g\,\mu_N\,k\,T)\,\langle v_{\mathrm{rel}}\rangle_0\,\mathfrak{S}(02) \tag{12b}$$

and
$$\eta(0) = k\,T/\langle v_{\mathrm{rel}}\rangle_0\,\mathfrak{S}(20)\,. \tag{13}$$

g is the molecular g-factor, μ_N the nuclear magneton, k Boltzmann's constant, T the absolute temperature, $\hbar$ Planck's constant and

$$\langle v_{\mathrm{rel}}\rangle_0 = (8\,k\,T/\pi\,\mu)^{1/2} \tag{14}$$

with μ the reduced mass. $(H/p)_{4/2}$ and $(H/p)_{\max}$ are the values for which the effects as described in Eqs. (9) and (10) reach half the saturation value and the maximum value respectively. The $\mathfrak{S}$'s are effective cross sections * given by [19]

$$\mathfrak{S}(20) = \frac{1}{\langle v_{\mathrm{rel}}\rangle_0}\,\frac{\langle [\boldsymbol{W}]^{(2)} : R_0[\boldsymbol{W}]^{(2)}\rangle_0}{\langle [\boldsymbol{W}]^{(2)} : [\boldsymbol{W}]^{(2)}\rangle_0}\,;$$

$$\mathfrak{S}(02) = \frac{1}{\langle v_{\mathrm{rel}}\rangle_0}\,\frac{\langle [\boldsymbol{J}]^{(2)} : R_0[\boldsymbol{J}]^{(2)}\rangle_0}{\langle [\boldsymbol{J}]^{(2)} : [\boldsymbol{J}]^{(2)}\rangle_0}\,;$$

$$\mathfrak{S}\left(\tfrac{02}{20}\right) = \frac{1}{\langle v_{\mathrm{rel}}\rangle_0}\,\frac{\langle [\boldsymbol{J}]^{(2)} : R_0[\boldsymbol{W}]^{(2)}\rangle_0}{\langle [\boldsymbol{J}]^{(2)} : [\boldsymbol{J}]^{(2)}\rangle_0^{1/2}\,\langle [\boldsymbol{W}]^{(2)} : [\boldsymbol{W}]^{(2)}\rangle_0^{1/2}} \tag{15}$$

R_0 is the collision superoperator defined by:

$$R_0\,\Phi = -(2\pi)^4\,\hbar^2\,n^{-1}\,\mathrm{tr}_1 \int \mathrm{d}\boldsymbol{p}_1\, f^{(0)}{}_1 \{\int t^g{}_{g'}(\Phi' + \Phi'_1)\, t^{g'}{}_g\, \delta(E)\,\mathrm{d}\boldsymbol{p}' - (i/2\pi)\,[t^g{}_g(\Phi + \Phi_1) - (\Phi + \Phi_1)\, t^g{}_g]\}\,. \tag{16}$$

For the meaning of the different symbols see for example Ref. [20]. $\mathfrak{S}(20)$ is the gas-kinetic viscosity cross section, $\mathfrak{S}(02)$ is the reorientation cross section for tensorial polarization of the rotational angular momentum and $\mathfrak{S}\left(\tfrac{02}{20}\right)$ is the cross section which describes the production of the angular momentum polarization from the polarization in the velocities. While $\mathfrak{S}(20)$ and $\mathfrak{S}(02)$ are positive, $\mathfrak{S}\left(\tfrac{02}{20}\right)$ can have either sign.

For HD the experimental results have been given for the quantities $[\eta_1^+ + \eta_2^+ - 2\eta(0)]/2\eta(0)$ and $(-\eta_1^+ + \eta_2^+)/2\eta(0))$ in the Figures 4 and 5.

In these Figures the theoretical curves are given by Eqs. (9) and (10) with $\mathfrak{S}(02)$ and $|\mathfrak{S}\left(\tfrac{02}{20}\right)|$ as adaptable parameters, for the position along the H/p axis and the magnitude of the effect. It is seen that for both combinations of coefficients the experimental data can be described very well with the theoretical expressions based on the $[\boldsymbol{J}]^{(2)}$ polarization only. At 77 K both combinations of coefficients have been measured. The results from both apparatuses can be described using a single set of values of the adaptable parameters (see Figure 6). From these results we draw two main conclusions: a) the results obtained with apparatus I and with apparatus II are consistent within the experimental accuracy, and b) the $[\boldsymbol{J}]^{(2)}$ polarization is by far dominant for HD in the whole temperature region.

The results for $[\eta_1^+ + \eta_2^+ - 2\eta(0)]/2\eta(0)$ obtained at various temperatures for the gases N_2, CO and CH_4 are given in Figures 7, 8 and 9. The theo-

* The shorthand notations $\mathfrak{S}\left(\tfrac{02}{20}\right)$, $\mathfrak{S}(02)$ and $\mathfrak{S}(20)$ corresponds to the full notations $\mathfrak{S}\left(\tfrac{0200}{2000}\right)$, $\mathfrak{S}\left(\tfrac{0200}{0200}\right)$ and $\mathfrak{S}\left(\tfrac{2000}{2000}\right)$ in more detailed discussions (see e.g. Table 2 in Ref. [18] and the appendix of Ref. [9]).

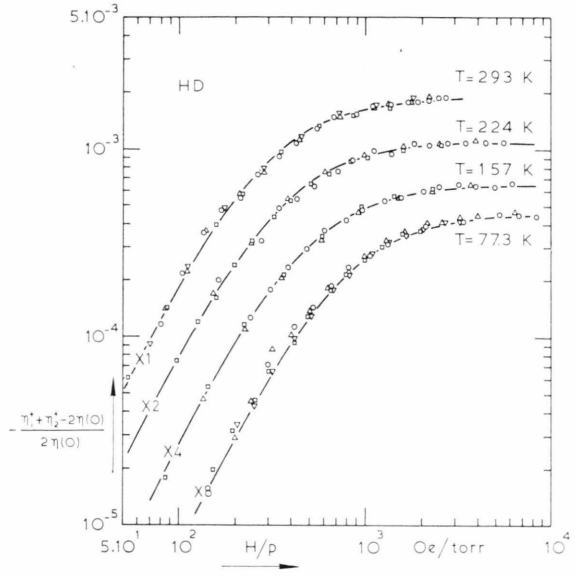

Fig. 4. $-[\eta_1^+ + \eta_2^+ - 2\,\eta(0)]/2\,\eta(0)$ versus H/p for HD at various temperatures. To distinguish the four different curves for 293 K, 224 K, 157 K and 77.3 K. They are vertically shifted by dividing them respectively by 1, 2, 4 and 8.
77.3 K: ○ 3.48 torr; △ 4.65 torr; ▽ 9.45 torr; □ 15.7 torr.
157 K: ○ 4.54 torr; △ 6.44 torr; □ 10.5 torr.
224 K: ○ 4.58 torr; △ 6.89 torr; □ 11.3 torr.
293 K: ○ 9.76 torr; △ 12.4 torr; ▽ 15.6 torr; □ 20.8 torr.
—— theoretical H/p dependence for $[\boldsymbol{J}]^{(2)}$ polarization, scaled to the experimental points.

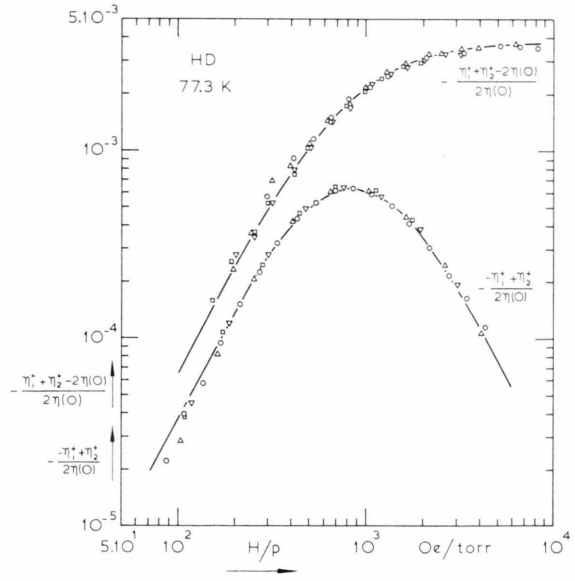

Fig. 6. $-[\eta_1^+ + \eta_2^+ - 2\,\eta(0)]/2\,\eta(0)$ and $-(-\eta_1^+ + \eta_2^+)/2\,\eta(0)$ versus H/p for HD at 77.3 K.
○△▽□ experimental points taken from Figures 4 and 5.
—— theoretical H/p dependence for $[\boldsymbol{J}]^{(2)}$ polarization, scaled to the experimental points.

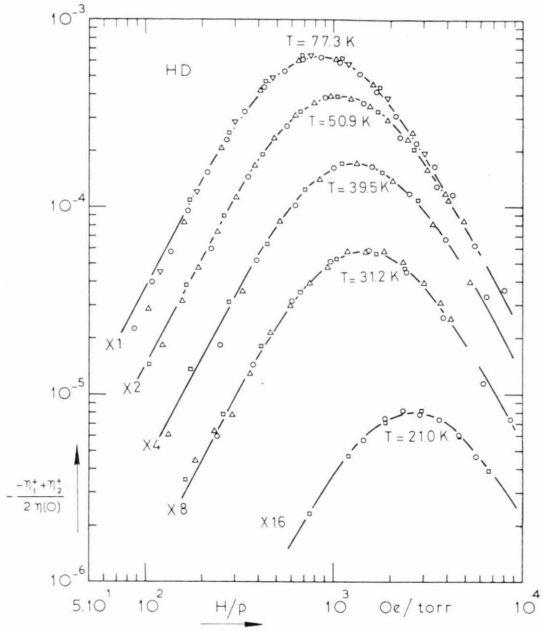

Fig. 5. $-(-\eta_1^+ + \eta_2^+)/2\,\eta(0)$ versus H/p for HD at various temperatures. To distinguish the different curves, they are shifted in the vertical direction as in Figure 4.
21.0 K: ○ 1.49 torr; □ 2.95 torr.
31.2 K: ○ 1.89 torr; △ 4.36 torr; □ 8.10 torr.
39.5 K: ○ 2.03 torr; △ 4.04 torr; □ 7.78 torr.
50.9 K: ○ 2.03 torr; △ 4.10 torr; □ 7.93 torr.
77.3 K: ○ 4.53 torr; △ 4.79 torr; ▽ 6.71 torr; □ 12.2 torr.
—— theoretical H/p dependence for $[\boldsymbol{J}]^{(2)}$ polarization, scaled to the experimental points.

retical curves have been given by Eq. (9) with $\Im(02)$ and $|\Im(^{02}_{20})|$ as adaptable parameters. It is seen that also here the experiments can be described with the theoretical expression. For N_2 and CO we also measured at 77 K the combination $(-\eta_1^+ + \eta_2^+)/2\,\eta(0)$. Here the results of the two experiments can also be described with one set of values for $\Im(02)$ and $|\Im(^{02}_{20})|$, see Figures 10 and 11. From these results it is concluded that the $[\boldsymbol{J}]^{(2)}$ polarization is dominant for all gases studied in the investigated temperature region.

The parameters $\Im(02)$ and $|\Im(^{02}_{20})|$ obtained for the different gases at different temperatures are given in Table 5. The values for $\Im(20)$ calculated using the literature values of $\eta(0)$ taken from Refs. [21] and [22] are also given. It is not possible from these experimnts [see Eq, (11)] to determine the sign of $\Im(^{02}_{20})$, which describes the orientation of the $[\boldsymbol{J}]^{(2)}$ polarization with respect to the $[\boldsymbol{W}]^{(2)}$ polarization. For N_2, CO and HD the sign of $\Im(^{02}_{20})$ is found to be positive from measurements of streaming birefrin-

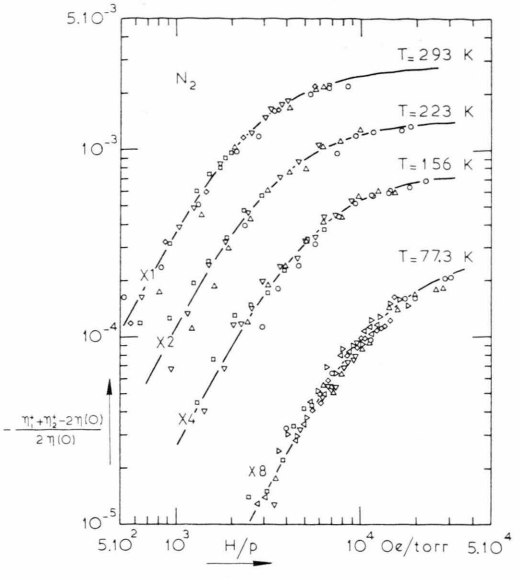

Fig. 7. $-[\eta_1^+ + \eta_2^+ - 2\eta(0)]/2\eta(0)$ versus H/p for N_2 at various temperatures. To distinguish the different curves, they are shifted in the vertical direction as in Figure 4.
77.3 K: ○ 0.966 torr; △ 1.09 torr; ▷ 1.72 torr; ◇ 2.04 torr; ◁ 2.48 torr; ▽ 3.29 torr; □ 5.08 torr.
156 K: ○ 1.31 torr; △ 1.96 torr; ▽ 3.43 torr; □ 4.95 torr.
223 K: ○ 1.61 torr; △ 2.45 torr; ▽ 4.25 torr; □ 8.44 torr.
293 K: ○ 3.61 torr; △ 4.60 torr; ◇ 5.39 torr; ▽ 7.61 torr; □ 15.5 torr.
—— theoretical H/p dependence for $[J]^{(2)}$ polarization, scaled to the experimental points.

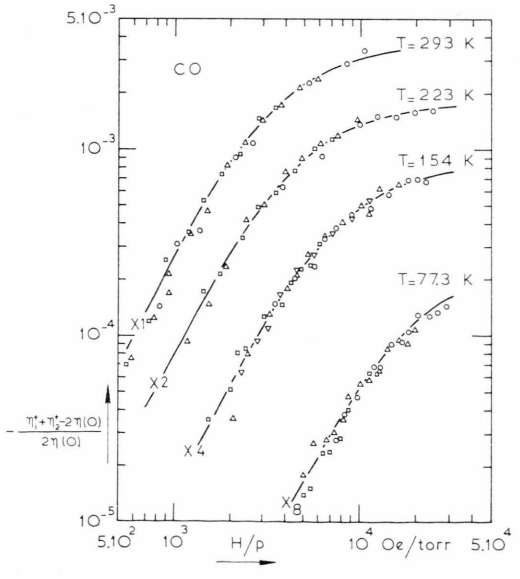

Fig. 8. $-[\eta_1^+ + \eta_2^+ - 2\eta(0)]/2\eta(0)$ versus H/p for CO at various temperatures. To distinguish the different curves, they are shifted in the vertical direction as in Figure 4.
77.3 K: ○ 1.03 torr; △ 1.53 torr; □ 2.49 torr.
154 K: ○ 1.32 torr; △ 1.88 torr; ▽ 2.71 torr; □ 5.12 torr.
223 K: ○ 1.18 torr; △ 2.54 torr; □ 4.38 torr.
293 K: ○ 2.89 torr; △ 5.20 torr; □ 8.79 torr.
—— theoretical H/p dependence for $[J]^{(2)}$ polarization, scaled to the experimental points.

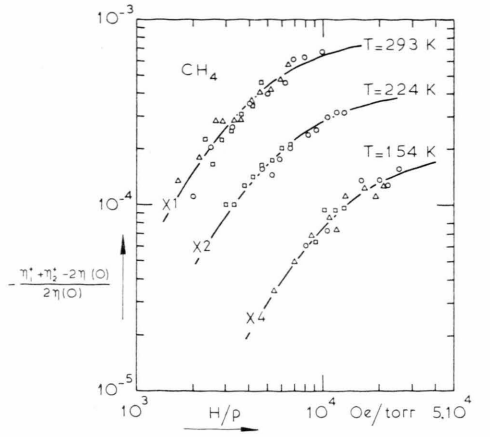

Fig. 9. $-[\eta_1^+ + \eta_2^+ - 2\eta(0)]/2\eta(0)$ versus H/p for CH_4 at various temperatures. To distinguish the different curves, they are shifted in the vertical direction as in Figure 4.
154 K: ○ 0.904 torr; △ 1.40 torr; □ 2.09 torr.
224 K: ○ 2.29 torr; □ 4.10 torr.
293 K: ○ 3.06 torr; △ 4.71 torr; □ 6.78 torr.
—— theoretical H/p dependence for $[J]^{(2)}$ polarization, scaled to the experimental points.

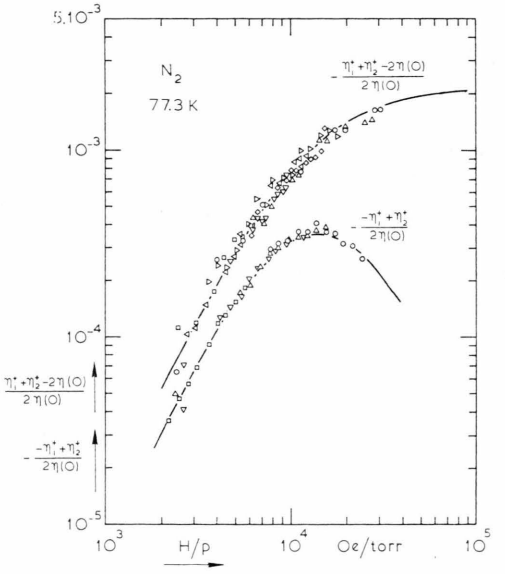

Fig. 10. $-[\eta_1^+ + \eta_2^+ - 2\eta(0)]/2\eta(0)$ and $-(-\eta_1^+ + \eta_2^+)/2\eta(0)$ versus H/p for N_2 at 77.3 K.
Upper curve: ○△▷◇◁▽□ points taken from Figure 7.
Lower curve: ○ 0.829 torr; △ 1.38 torr; ▽ 2.03 torr; □ 3.90 torr.
—— theoretical H/p dependence for $[J]^{(2)}$ polarization, scaled to the experimental points.

gence which have been performed by Baas [23]. Plots of the cross sections $\mathfrak{S}(02)$ and $|\mathfrak{S}(^{02}_{20})|$ for HD, N_2, CO and CH_4 versus the temperature are given in the Figures 12 to 15. For comparison the gas-kinetic viscosity cross section $\mathfrak{S}(20)$ is also given. From the relatively small values of $\mathfrak{S}(02)$ with respect to $\mathfrak{S}(20)$ it is found that HD collisions are rather ineffective in reorienting a molecule. The plot for $|\mathfrak{S}(^{02}_{20})|$ shows for HD a cross section which at first increases with decreasing temperature, and then

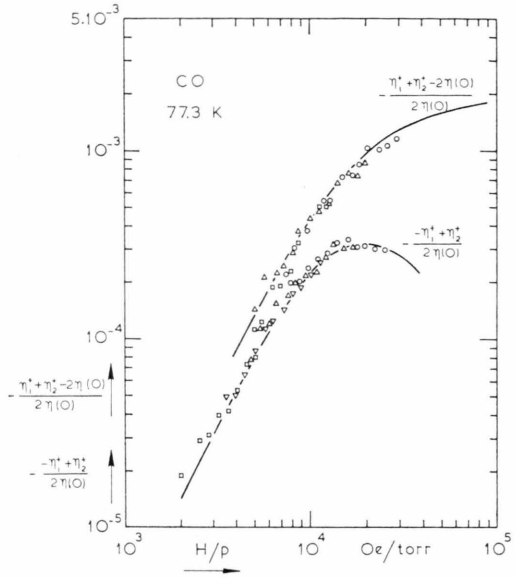

Fig. 11. $-[\eta_1^+ + \eta_2^+ - 2\eta(0)]/2\eta(0)$ and $-(-\eta_1^+ + \eta_2^+)/2\eta(0)$ versus H/p for CO at 77.3 K.
Upper curve: ○△□ points taken from Figure 8.
Lower curve: ○ 0.802 torr; △ 1.22 torr; ▽ 1.89 torr; □ 4.33 torr.
—— theoretical H/p dependence for $[J]^{(2)}$ polarization, scaled to the experimental points.

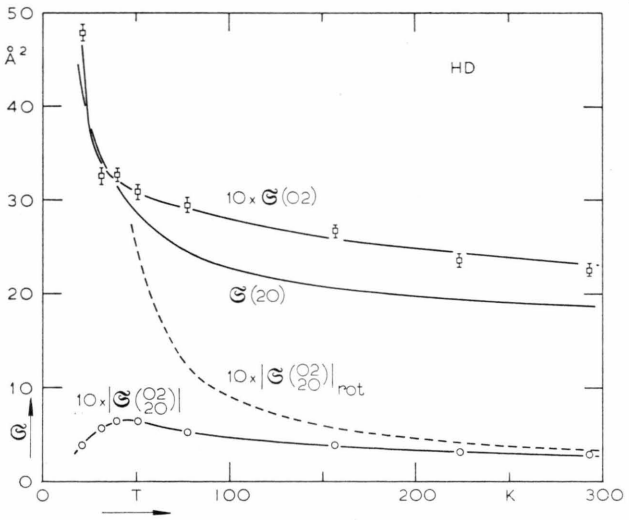

Fig. 12. Effective cross sections for HD versus temperature. For the dotted line which represents $|\mathfrak{S}^{(02)}_{(20)\,\mathrm{rot}}|$, see text.

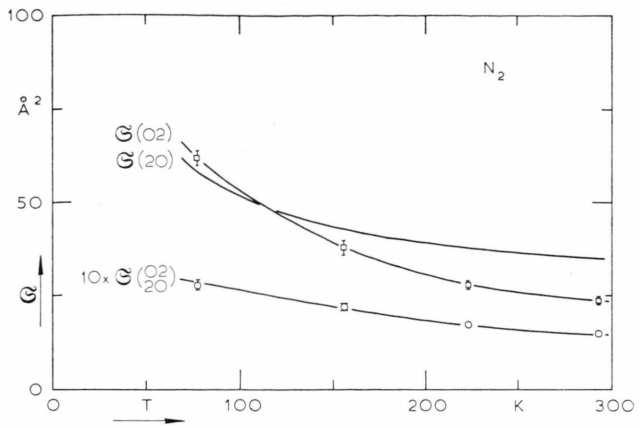

Fig. 13. Effective cross sections for N_2 versus temperature.

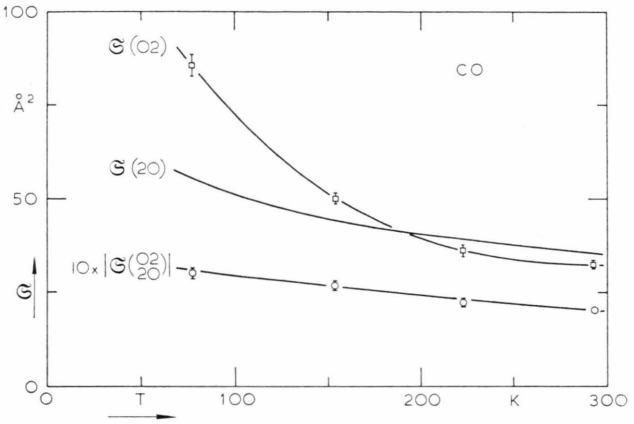

Fig. 14. Effective cross sections for CO versus temperature.

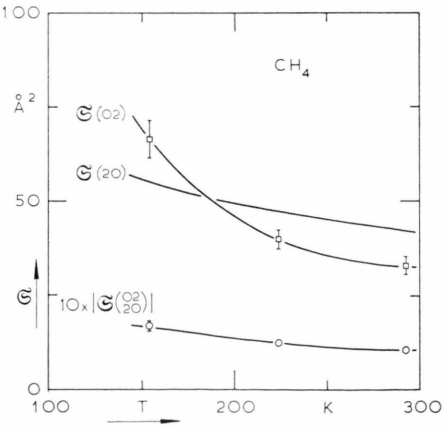

Fig. 15. Effective cross sections for CH_4 versus temperature.

below 45 K begins to decrease rapidly. This behaviour at the lower temperatures can be explained by the fact that molecules in the rotational state $J=0$ do not contribute to the field effect. If HD in the $J=0$ rotational state can be considered a "noble" gas as far as these experiments are concerned, then the expression for mixtures can be used (see Ref. [24]). This mixture is composed of rotating ($J \neq 0$) and non-rotating ($J=0$) HD molecules, and the follow-

Table 4.

T (K)	$(H/p)_{max}$, $(H/p)_{1/2}$ (kOe/torr)	$\eta(0)\times10^6$ [22] (P)	$\Psi_{02}\times10^3$
HD			
21.0	2.65±0.05	13.0±0.1	0.78±0.02
31.2	1.48±0.04	18.4±0.2	2.75±0.08
39.5	1.32±0.03	23.4±0.2	4.0 ±0.1
50.9	1.10±0.03	29.3±0.3	4.6 ±0.1
77.3	0.85±0.02	42.0±0.4	3.8 ±0.1
77.3	0.85±0.02	42.0±0.4	3.7 ±0.1
157	0.54±0.02	70.9±0.7	2.62±0.06
224	0.40±0.02	89.7±0.9	2.20±0.06
293	0.33±0.01	107 ±1	1.87±0.04
N_2			
77.3	14.0 ±0.5	54.3±0.5	2.2 ±0.1
77.3	14.0 ±0.5	54.3±0.5	2.1 ±0.1
156	6.0 ±0.3	104 ±1	3.0 ±0.1
223	3.7 ±0.3	141 ±1	2.8 ±0.1
293	2.76±0.07	174 ±2	2.7 ±0.1
CO			
77.3	19.8 ±0.8	56.6±0.6	1.9 ±0.1
77.3	20.0 ±0.8	56.6±0.6	1.9 ±0.1
154	8.3 ±0.3	100 ±1	3.3 ±0.1
223	5.0 ±0.2	136 ±1	3.5 ±0.1
293	3.89±0.08	172 ±2	3.6 ±0.1
CH_4			
154	13 ±0.7	60.7±0.6	0.75±0.06
224	6.2±0.4	85.6±0.9	0.81±0.04
293	4.5±0.5	109 ±1	0.80±0.04

ing expressions are obtained:

$$\Psi_{02}=x\,\frac{\{x\,\Im(^{02}_{20})_{rot}+(1-x)\,\Im(^{02}_{20})_{rot-n.rot}\}^2}{\{x\,\Im(02)_{rot}+(1-x)\,\Im(02)_{rot-n.rot}\}\,\Im(20)} \tag{17}$$

and

$$\xi_{02}=\frac{1}{\langle v_{rel}\rangle_0\{x\,\Im(02)_{rot}+(1-x)\,\Im(02)_{rot-n.rot}\}\,\frac{g\,\mu_N\,k\,T}{\hbar}\,\frac{H}{p}}\cdot \tag{18}$$

The quantity $\Im(^{02}_{20})_{rot}$ gives the production of $[\boldsymbol{J}]^{(2)}$ polarization from the $[\boldsymbol{W}]^{(2)}$ polarization while

Table 5.

T (K)	$\Im(02)$ (Å²)	$\Im(20)$ (Å²)	$\Im(^{02}_{20})$ (Å²)
HD			
21.0	4.79±0.09	41.3±0.4	0.39±0.01
31.2	3.26±0.09	35.6±0.4	0.57±0.02
39.5	3.27±0.07	31.5±0.3	0.64±0.02
50.9	3.09±0.08	28.5±0.3	0.64±0.02
77.3	2.95±0.08	24.5±0.2	0.52±0.02
157	2.67±0.07	20.7±0.2	0.38±0.01
224	2.36±0.07	19.5±0.2	0.32±0.01
293	2.26±0.07	18.7±0.2	0.28±0.01
N_2			
77.3	62 ±2	57.7±0.6	2.8 ±0.1
156	38 ±2	42.6±0.4	2.2 ±0.1
223	28 ±1	37.7±0.4	1.71±0.07
293	24 ±1	35.0±0.4	1.49±0.05
CO			
77.3	86 ±3	55.3±0.6	3.0 ±0.1
154	50 ±2	44.1±0.4	2.70±0.09
223	36 ±1	39.1±0.4	2.23±0.09
293	32.5 ±0.8	35.5±0.4	2.04±0.06
CH_4			
154	67 ±5	55.1±0.6	1.7 ±0.1
224	40 ±3	47.1±0.5	1.23±0.08
293	33 ±2	42.4±0.4	1.06±0.07

$\Im(02)_{rot}$ describes the reorientation of the $J\neq0$ molecules. $\Im(^{02}_{20})_{rot-n.rot}$ and $\Im(02)_{rot-n.rot}$ give the production of $[\boldsymbol{J}]^{(2)}$ polarization and the reorientation of the molecules in a gas in which the rotating molecules are infinitely diluted. The quantity x is the fraction of rotating molecules which can be calculated by $x=\sum_{J\neq0}P_J$ where P_J is the fractional population of the J state given by:

$$P_J=\frac{(2J+1)\,\exp\{-J(J+1)\,\Theta/T\}}{\sum_J(2J+1)\,\exp\{-J(J+1)\,\Theta/T\}}\,. \tag{19}$$

For HD ($\Theta=63.8$ K) the occupation of the different rotational levels as a function of the temperature is illustrated in Figure 16. Under certain as-

sumptions with respect to $\mathfrak{S}(^{02}_{20})_{\text{rot-n.rot}}$ the quantity $|\mathfrak{S}(^{02}_{20})_{\text{rot}}|$ can be obtained as a function of temperature. In Fig. 12 $|\mathfrak{S}(^{02}_{20})_{\text{rot}}|$ is plotted for the rather arbitrary choice of $\mathfrak{S}(^{02}_{20})_{\text{rot-n.rot}} = \frac{1}{2}\mathfrak{S}(^{02}_{20})_{\text{rot}}$. This assumption seems reasonable in comparison with the experiments done on mixtures with noble gases [24]. It is seen that the dependence on temperature of $|\mathfrak{S}(^{02}_{20})_{\text{rot}}|$ for HD does not essentially differ from that for $|\mathfrak{S}(^{02}_{20})|$ of the gases N_2, CO and CH_4 which have smaller rotational constants.

For the gases N_2, CO and CH_4 the reorientation cross section $\mathfrak{S}(02)$ has a steep temperature dependence and becomes at lower temperatures even larger than the gas-kinetic cross section. Furthermore, the fact that the cross section $|\mathfrak{S}(^{02}_{20})|$ is always much smaller than $\mathfrak{S}(02)$ means that the collisions are not very effective in producing a $[\boldsymbol{J}]^{(2)}$ polarization from a $[\boldsymbol{W}]^{(2)}$ polarization. Note that the field strength is always so high that the nuclear spin and the magnetic moment of the molecule are completely decoupled, so that the presence of the nuclear spin can be neglected in the magnetic field effects.

To get a better idea of the temperature dependence of the reorientation cross section of the gases N_2 and CO a plot is made of $\mathfrak{S}(02)$ versus T^{-1}, see Figure 17. It is seen that the temperature dependence in the investigated region can be described by:

$$\mathfrak{S}(02) = a + b\,T^{-1} \tag{20}$$

with $a = 10$ Å^2 and $b = 41 \times 10^2$ Å^2 K for N_2 while $a = 13.5$ Å^2 and $b = 55 \times 10^2$ Å^2 K for CO.

We will now compare our results at room temperature with the results of Refs. [8, 9, 11]. In Table 6 values for $\mathfrak{S}(02)$ and $|\mathfrak{S}(^{02}_{20})|$ from the different experiments are given for HD, N_2, CO and CH_4. Good agreement is found. The fact that our $\mathfrak{S}(02)$ is somewhat larger than that of the other experiments is caused by a slightly different interpretation of the experimental results: we take the best fit of the theoretical curves over the whole H/p domain, while Korving [11] and Hulsman [8, 9] favour the lower H/p values.

Table 6. Comparison with other data at room temperature.

	$\mathfrak{S}(02)$ (Å^2)				$\lvert\mathfrak{S}(^{02}_{20})\rvert$ (Å^2)	
	this research	Ref. [8]	Ref. [9]	Ref. [11]	this research	Ref. [9]
HD	2.26 ± 0.07	2.3	2.2	—	0.282 ± 0.009	0.28
N_2	23.7 ± 0.9	22	22	21	1.49 ± 0.05	1.46
CO	32.5 ± 0.8	31	31	31	2.04 ± 0.06	1.97
CH_4	33.0 ± 2.5	32	30	32	1.06 ± 0.07	1.01

5. A Comparison with Nuclear Magnetic Relaxation (NMR) Experiments

Also from NMR, molecular cross sections can be obtained which are related to the reorientation of the molecules. Hence it is useful to compare $\mathfrak{S}(02)$ obtained from our experiments with the NMR cross sections. First we will summarize the different mechanisms that can cause relaxation of the nuclear spin in diatomic molecules and in spherical top molecules. Only the extreme narrowing limit is considered.

5.1. Survey of relaxation mechanisms.

Diatomic molecules. In dilute gases of diatomic molecules three kinds of intramolecular relaxation can be distinguished.

Spin-rotation interaction: Nuclear spins may relax through an interaction with the rotational motion of the molecule which causes a local magnetic field at the site of a nucleus. Starting from the Waldmann-Snider equation Chen and Snider [25] derived an expression for the relaxation times T_1 and T_2 in which the decay time is given explicitly in terms of a two particle collision integral. For a single rotational level with quantum number J it is found that

$$T_1^{-1} = T_2^{-1} = \tfrac{2}{3}\,c^2\,J(J+1)\,\tau_1\,. \tag{21}$$

Here c is the spin-rotation coupling constant and τ_1 is the decay time for vectorial polarization of the rotational angular momentum J. It is

$$\tau_1^{-1} = \langle \boldsymbol{J}\cdot R_0'\,\boldsymbol{J}\rangle_0 / J(J+1) \tag{22}$$

where R_0' is the collision superoperator defined as:

$$\begin{aligned} R_0'\,\Phi = &-(2\pi)^4\,\hbar\,n^{-1}\,\mathrm{tr}_1 \\ &\int \mathrm{d}\boldsymbol{p}_1\, f_1^{(0)}\,\{\int t^g{}_{g'}(\Phi')\,t^{g^+}{}_{g'}\,\delta(E)\,\mathrm{d}\boldsymbol{p}' \\ &-(i/2\pi)\,[t^g{}_{g'}(\Phi) - (\Phi)\,t^{g^+}{}_g]\}\,. \end{aligned} \tag{23}$$

(The collision superoperator defined here differs from that given in Eq. (16) in that the collision partner does not explicitly appear in R_0'. This is a consequence of assuming that collisions cannot change nuclear spin states.)

For the meaning of the various symbols see Refs. [20] and [25].

Dipole-dipole interaction: The nuclear spins may relax through mutual interaction of the nuclear spins in the same molecule. For this intramolecular process Chen and Snider give expressions for the relaxation times of a single J-level system, which is valid for

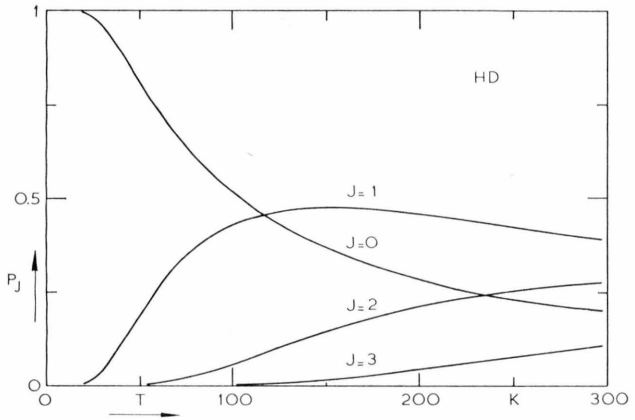

Fig. 16. The populations of different rotational levels for HD versus temperature.

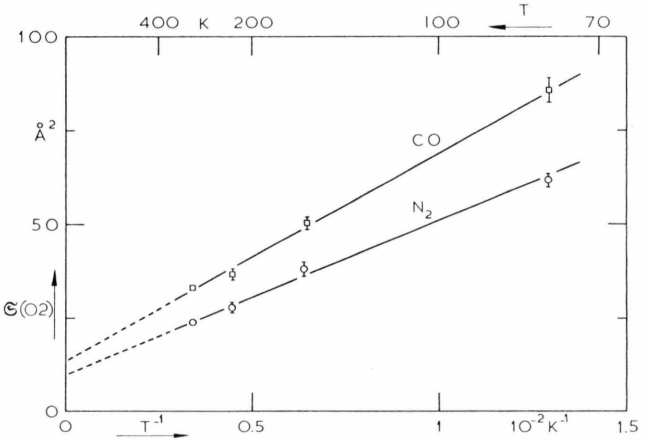

Fig. 17. The reorientation cross section for tensorial polarization $\mathfrak{S}(02)$ versus T^{-1} for N_2 and CO.

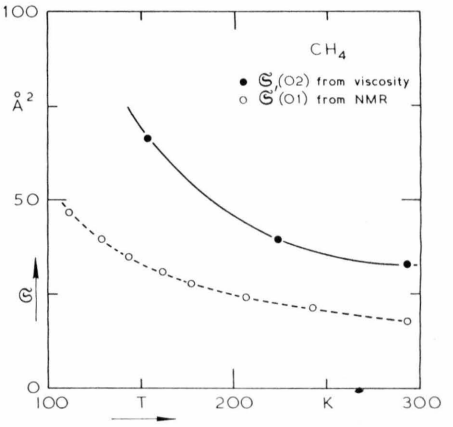

Fig. 20. Comparison for CH_4 between $\mathfrak{S}(02)$ from our experiments and $\mathfrak{S}(01)$ obtained from NMR.

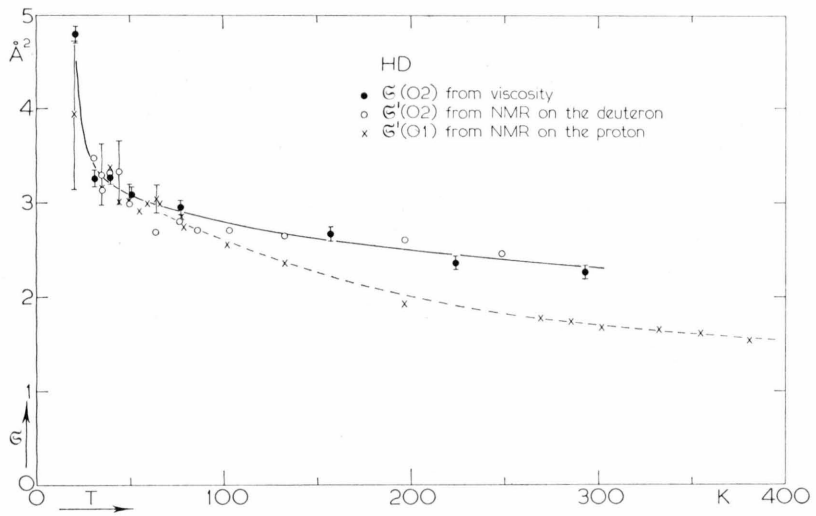

Fig. 18. Comparison for HD between $\mathfrak{S}(02)$ from our experiments and $\mathfrak{S}'(01)$ and $\mathfrak{S}'(02)$ obtained from NMR.

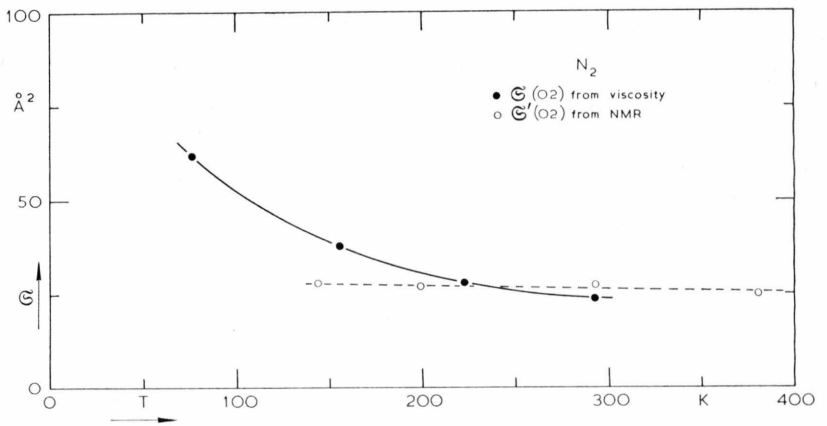

Fig. 19. Comparison for N_2 between $\mathfrak{S}(02)$ from our experiments and $\mathfrak{S}'(02)$ obtained from NMR.

$I=\frac{1}{2}$:

$$T_1^{-1}=T_2^{-1}=\frac{2}{15}\,c_d^2\,\frac{J(J+1)}{(2J-1)(2J+3)}\,(2I-1)(2I+3)\,a_l^2\,\tau_2 \tag{24}$$

where I is the total spin of the molecule. a_l is given by:

$$a_l=\frac{I^2(I+1)^2-3[I_1(I_1+1)-I_2(I_2+1)]^2+2I(I+1)\,[I_1(I_1+1)+I_2(I_2+1)]}{2I(I+1)(2I-1)(2I+3)}$$

and $c_d=-6\,g_l^2\,\mu_N^2/2\hbar\,r^3$, where g_l is the nuclear g-factor and r is the distance between the two nuclei which, in general, have different spins $\boldsymbol{I}_1$ and $\boldsymbol{I}_2$. The decay time τ_2 for this mechanism is given in terms of collision integrals of the $[\boldsymbol{J}]^{(2)}$ rotational angular momentum:

$$\tau_2^{-1}=\frac{\langle[\boldsymbol{J}]^{(2)}:R_0'[\boldsymbol{J}]^{(2)}\rangle_0}{\frac{1}{6}J(J+1)(2J-1)(2J+3)} \tag{25}$$

Quadrupole interaction: The nuclear spins may relax through interaction with the electric-field gradients of the molecule, if the nuclei possess a quadrupole moment. This occurs only for nuclei with spin greater than 1/2 and when present it is the dominant mechanism. This type of relaxation has not been discussed by Chen and Snider. Formally, however, the problem is quite analogous to the dipole-dipole situation. For quadrupole relaxation in diatomics two different cases have to be distinguished, i. e., a) molecules in which only one of the nuclei is of importance for the relaxation and b) molecules in which both nuclei are identical and have spins greater than 1/2. For the molecules of type a), we find for a single level system:

$$T_1^{-1}=T_2^{-1}=\frac{3}{40}\,\frac{J(J+1)}{(2J-1)(2J+3)}\,\frac{2I_1+3}{I_1^2(2I_1-1)}\cdot(e\,q\,Q/\hbar)^2\,\tau_2 \tag{26}$$

where τ_2 is the same quantity that occurs for the dipole-dipole relaxation given in Eq. (25), I_1 is the spin quantum number of the relevant nucleus and $e\,q\,Q/\hbar$ the intramolecular quadrupole coupling constant. For molecules having two identical nuclei of spin 1 it is found that (see also Ref. [26]) both the ortho and the para system have the same relaxation time T_1:

$$T_1^{-1}=T_2^{-1}=\frac{3}{40}\,\frac{J(J+1)}{(2J-1)(2J+3)}\,5\,(e\,q\,Q/\hbar)^2\,\tau_2\,. \tag{27}$$

Multilevel system: To describe nuclear spin relaxation when many rotational levels are involved, some appropriate averaging must be introduced. By treating τ_1 and τ_2 as effective decay or correlation times, a simple Boltzmann averaging can be used, viz.

$$T_1^{-1}=T_2^{-1}=\tfrac{2}{3}\,c^2\langle J(J+1)\rangle_0\,\tau_1\,, \tag{28}$$

$$T_1^{-1}=T_2^{-1}=\frac{2}{15}\,c_d^2\left\langle\frac{J(J+1)}{(2J-1)(2J+3)}\,(2I-1)(2I+3)\,a_l^2\right\rangle_0\tau_2\,, \tag{29}$$

$$T_1^{-1}=T_2^{-1}=\frac{3}{40}\left\langle\frac{J(J+1)}{(2J-1)(2J+3)}\,\frac{2I_1+3}{I_1^2(2I_1-1)}\right\rangle_0(e\,q\,Q/\hbar)^2\,\tau_2\,, \tag{30}$$

$$T_1^{-1}=T_2^{-1}=\frac{3}{40}\left\langle\frac{J(J+1)}{(2J-1)(2J+3)}\right\rangle_0 5\,(e\,q\,Q/\hbar)^2\,\tau_2 \tag{31}$$

for respectively spin-rotation, dipole-dipole and two cases of quadrupole relaxation in diatomic molecules (see also Ref. [27]). Note that for high J values Eqs. (28) and (30), (29) and (31) agree with the classical treatment of Gordon [28].

Spherical top molecules: For spherical top molecules as CH_4, CF_4 and CD_4 the relaxation mechanisms which are of importance are:

Spin-rotation interaction: This relaxation mechanism in spherical tops is treated by Dong and Bloom [29] and McCourt and Hess [30]. The relaxation times are given by:

$$T_1^{-1}=T_2^{-1}=\frac{2}{3}\,\frac{\langle J(J+1)\,I(I+1)\rangle_0}{\langle I(I+1)\rangle_0}\,\{c_a^2+\tfrac{4}{45}c_d^2\}\,\tau_1 \tag{32}$$

where I is the total spin, c_a and c_d are two independent coupling constants by which the spin-rotation interaction can be characterized. The quantity $\langle J(J+1)\, I(I+1)\rangle_0 / \langle I(I+1)\rangle_0$ can be calculated using the results of Refs. [31] and [32]. For temperatures which are not too low (>100 K) it is equal to $3\, I_0\, k\, T/\hbar^2$ where I_0 is the moment of inertia.

Quadrupole interaction: For this mechanism in spherical top molecules an expression is given by Bloom et al. [33] using a correlation function approach which gives:

$$T_1^{-1} = T_2^{-1} = \tfrac{3}{8}\,(e\,q\,Q/\hbar)^2\, f_2\, \tau_2 \qquad (33)$$

with $f_2 = 0.2$ for spherical top molecules.

5.2. Comparison of cross sections

To compare the NMR data with our results we introduce also (effective) cross sections for NMR by:

$$\tau_i^{-1} = n \langle v_{rel}\rangle_0\, \mathfrak{S}'(0i) \qquad (34)$$

where $i = 1$ for spin-rotation and $i = 2$ for dipole-dipole and quadrupole relaxation. The prime refers to the collision superoperator which for NMR is different from that used in the viscosity cross sections, see Equations (16) and (23). Thus the NMR cross sections are given by:

$$\mathfrak{S}'(01) = \frac{1}{\langle v_{rel}\rangle_0}\, \frac{\langle \boldsymbol{J}\cdot R_0'\, \boldsymbol{J}\rangle_0}{\langle \boldsymbol{J}\cdot\boldsymbol{J}\rangle_0},$$

$$\mathfrak{S}'(02) = \frac{1}{\langle v_{rel}\rangle_0}\, \frac{\langle [\boldsymbol{J}]^{(2)} : R_0'\, [\boldsymbol{J}]^{(2)}\rangle_0}{\langle [\boldsymbol{J}]^{(2)} : [\boldsymbol{J}]^{(2)}\rangle_0}. \qquad (35)$$

Now we will treat successively the gases HD, N_2, CH_4, CF_4 and CD_4.

Hydrogen deuteride: It is possible to obtain from NMR experiments on HD both $\mathfrak{S}'(01)$ and $\mathfrak{S}'(02)$. In Fig. 18 these quantities are calculated from the measurements done by Hardy [34] and compared with $\mathfrak{S}(02)$ from the field effect on viscosity. It can be seen that within the accuracy of both experiments $\mathfrak{S}(02)$ and $\mathfrak{S}'(02)$ are equal. From this result it can be concluded that there is no direct transfer of $[\boldsymbol{J}]^{(2)}$ polarization during a collision. This is in agreement with a conclusion of the distorted wave Born approximation as used by Chen, Moraal and Snider [35] [see their Equation (92)]. $\mathfrak{S}'(01)$ is for lower temperatures close to $\mathfrak{S}'(02)$ while for higher temperatures it becomes smaller than $\mathfrak{S}'(02)$. The ratio $\mathfrak{S}'(02)/\mathfrak{S}'(01)$ varies from 1 to 1.35 in agreement with the appropriate limits $(1 < \tau_1/\tau_2 < 3)$ given by Bloom and Oppenheim [33].

Nitrogen: NMR measurements on N_2 have been performed by Speight and Armstrong [36] at rather high densities (100 – 600 amagat). The $\mathfrak{S}'(02)$ cross section calculated from these experiments using Eqs. (31) and (34) is plotted in Fig. 19 together with $\mathfrak{S}(02)$. A great discrepancy between both experiments is found. Since the densities are high in the NMR experiment, the gas may not be considered dilute, which may account for the disagreement. From this point of view NMR experiments for N_2 at lower densities are desirable.

Methane: For CH_4 the spin-rotation mechanism is dominant giving the $\mathfrak{S}'(01)$ cross section from NMR measurements. Using the data of Ref. [33], this cross section is compared with our $\mathfrak{S}(02)$ in Figure 20. The ratio $\mathfrak{S}(02)/\mathfrak{S}'(01)$ is about 1.85 for all temperatures.

Tetrafluoromethane: For CF_4 field dependent viscosity measurements have been performed at room temperature by Korving [11] and Hulsman et al. [9]. With these results and those obtained from the NMR measurements of Dong and Bloom [29] for $\mathfrak{S}'(01)$, we find that the ratio $\mathfrak{S}(02)/\mathfrak{S}'(01)$ is about 1.6.

Tetradeuteromethane: In CD_4 relaxation occurs through a quadrupole mechanism. The coupling constant $e\,q\,Q/\hbar$ for this gas, however, is not known experimentally. Using estimated values as given in Ref. [33] the $\mathfrak{S}'(02)$ cross section at room temperature obeys the following inequality:

$$21\ \text{Å}^2 \leqq \mathfrak{S}'(02) \leqq 49\ \text{Å}^2.$$

The value of $\mathfrak{S}(02)$ obtained from the viscosity experiments of Korving et al. [10] is 21 Å^2, from which it can be concluded that the two experiments are in agreement.

For completeness the various parameters used in the calculations of the NMR cross sections are given in Table 7.

Table 7. Summary of the molecular parameters used in the calculations of the NMR cross sections.

	$c^2 \times 10^{-10}$ $(c_a^2 + \frac{4}{45} c_d^2) \times 10^{-10}$ (rad^2 sec^{-2})	$(e\,q\,Q/\hbar)^2 \times 10^{-10}$ (rad^2 sec^{-2})
HD	30.0	203
N_2		121×10^3
CH_4	0.54	
CF_4	0.16	
CD_4		66–159

Similar information on reorientation of molecules can be obtained from depolarized Rayleigh light scattering experiments. A comparison between results of these experiments and those discussed here will be given in Ref. [37].

Acknowledgements

We greatefully acknowledge stimulating discussions with Dr. B. C. Sanctuary.

This work is part of the research program of the "Stichting voor Fundamenteel Onderzoek der Materie (F.O.M.)" and has been made possible by financial support from the "Nederlandse Organisatie voor Zuiver Wetenschappelijk Onderzoek (Z.W.O.)".

[1] J. J. M. Beenakker, Festkörperprobleme VIII, ed. O. Madelung, Vieweg Verlag, Braunschweig 1968, p. 276.
[2] J. J. M. Beenakker and F. R. McCourt, Ann. Rev. Phys. Chem. **21**, 47 [1970].
[3] G. J. Hooyman, P. Mazur, and S. R. De Groot, Physica **21**, 355 [1955].
[4] S. R. De Groot and P. Mazur, Non-equilibrium Thermodynamics, North-Holland Publishing Comp., Amsterdam 1962, p. 311.
[5] J. A. R. Coope and R. F. Snider, J. Chem. Phys. **56**, 2056 [1972].
[6] S. Hess and L.Waldmann, Z. Naturforsch. **26 a**, 1057 [1971].
[7] H. Hulsman and A. L. J. Burgmans, Phys. Letters **29 A**, 629 [1969].
[8] H. Hulsman, E. J. van Waasdijk, A. L. J. Burgmans, H. F. P. Knaap, and J. J. M. Beenakker, Physica **50**, 53 [1970] (Commun. Kamerlingh Onnes Lab, Leiden No. 381 c).
[9] H. Hulsman, F. G. van Kuik, K. W. Walstra, H. F. P. Knaap, and J. J. M. Beenakker, Physika **57**, 501 [1972].
[10] J. Korving, H. Hulsman, G. Scoles, H. F. P. Knaap, and J. J. M. Beenakker, Physica **36**, 177 [1967] (Commun. Kamerlingh Onnes Lab., Leiden No. 357 b).
[11] J. Korving, Physica **50**, 27 [1970] (Commun. Kamerlingh Onnes Lab., Leiden No. 381 b).
[12] H. van Ee, Thesis Leiden, p. 21 (1966).
[13] H. Hulsman and H. F. P. Knaap, Physica **50**, 565 [1970] (Commun. Kamerlingh Onnes Lab., Leiden No. 383 b).
[14] J. O. Hirschfelder, C. F. Curtiss, and R. B. Bird, Molecular theory of gases and liquids, John Wiley, New York 1954, p. 545.
[15] F. Kohlrausch, Praktische Physik, B. G. Teubner Verlagsgesellschaft, Stuttgart 1968, Band I, p. 178.
[16] L. B. Loeb, The kinetic theory of gases, McGraw-Hill Book Cy., Inc., New York and London 1934, p. 297.
[17] H. Moraal, F. R. McCourt, and H. F. P. Knaap, Physica **45**, 455 [1969] (Commun. Kamerlingh Onnes Lab., Leiden, Suppl. No. 127 d).
[18] G. J. Prangsma, A. L. J. Burgmans, H. F. P. Knaap, and J. J. M. Beenakker, Physica, to be published [1973].
[19] F. R. McCourt and H. Moraal, Chem. Phys. Letters **9**, 39 [1971].
[20] A. C. Levi, F. R. McCourt, and A. Tip, Physica **39**, 165 [1968] (Commun. Kamerlingh Onnes Lab., Leiden, Suppl. No. 126 b).
[21] Data Book, edited by Thermophysical Properties Research Center, Purdue University, Lafayette, Indiana 1966, Vol. 2.
[22] A. O. Rietveld, A. van Itterbeek, and C. A. Velds, Physica **25**, 205 [1959] (Commun. Kamerlingh Onnes Lab., Leiden, No. 314 b).
[23] F. Baas, Phys. Letters **36 A**, 107 [1971]; F. Baas, private communication.
[24] A. L. J. Burgmans, P. G. van Ditzhuyzen, and H. F. P. Knaap, Z. Naturforsch. **28 a**, 849 [1973].
[25] F. M. Chen and R. F. Snider, J. Chem. Phys. **48**, 3185 [1968].
[26] M. Bloom, private communication. — M. Bloom, M. T. P. International Review of Science, Physical Chemistry Section, Vol. 4, ed. C. A. McDowell (Medical and Technical Publishing Co., Oxford, England 1973). — B. C. Sanctuary, to be published.
[27] M. Bloom and I. Oppenheim, Adv. Chem. Phys. **12**, 549 [1967].
[28] R. G. Gordon, J. Chem. Phys. **44**, 228 [1966].
[29] R. Y. Dong and M. Bloom, Canad. J. Phys. **48**, 793 [1970].
[30] F. R. McCourt and S. Hess, Z. Naturforsch. **26 a**, 1234 [1971].
[31] P. Yi, I. Ozier, and C. H. Anderson, Phys. Rev. **165**, 92 [1968].
[32] E. Bright Wilson, Jr., J. Chem. Phys. **3**, 276 [1935].
[33] M. Bloom, F. Bridges, and W. N. Hardy, Canad. J. Phys. **45**, 3533 [1967].
[34] W. N. Hardy, Thesis Vancouver (1964).
[35] F. M. Chen, H. Moraal, and R. F. Snider, J. Chem. Phys. **57**, 542 [1972].
[36] P. A. Speight and R. L. Armstrong, Canad. J. Phys. **47**, 1475 [1969].
[37] R. A. J. Keijser et al., Physica, to be published.